International Journal of Scientific Research in Mechanical and Materials Engineering
© 2019 IJSRMME | ISSN : 2457-0435

A Study on the Dynamic Analysis Modelling for High-Speed Roller Bearings

CholUk Ri, ZhunHyok Zhang, WonRyong Pak, JaeHun Kim, IlSon Yun, CholMin Han, JongMin Han
Kim Chaek University of Technology, School of Mechanical Science and Technology, Pyongyang, Democratic People's Republic of Korea

Article Info
Volume 5, Issue 1
Page Number : 01-10
Publication Issue :
January-February-2021

Article History
Accepted : 15 Jan 2021
Published : 27 Jan 2021

ABSTRACT

High-speed roller bearings are widely used in the aerospace field due to their importance. As rotating machinery develops in the areas of high speed, high precision, and high reliability, research on the dynamic performance of roller bearings is becoming more and more important. Constructing a dynamic analysis model accurately is very important in interpreting his dynamic characteristics. The basis for dynamic analysis of high-speed rolling bearings is the creation of a dynamic model of the bearing. In this paper, the method of creation dynamic analysis model of high-speed roller bearings was studied specifically. First, based on the Gupta model for high-speed roller bearings, a model was created that considered the effects of viscous resistance and oil film resistance, frictional relationship, and contact force action between the rolling element and cage. In addition, it specifically analyzed the forces and kinematic relations of each part within the rolling bearing. The dynamic model of the high-speed roller bearing was built based on the specific consideration of the factors affecting the bearing rotor system, such as load, speed, gap, friction, and resistance forces, and based on creating the dynamic equation of each part, the dynamic model of high-speed roller bearing was established.

Keywords : Roller bearing, Dynamic model, Simulation analysis, Viscosity resistance, Oil film resistance

I. INTRODUCTION

Roller bearings are important supporting parts that receive transmission movements and loads in various rotating machines, which relies on the contact between the parts to support the rotating part. It is widely used in precision machinery, aerospace, automobile industry, machine tools, and robots, as it has advantages such as small friction, easy to maneuver, easy to lubricated, and easy to replace. Roller bearings applied in the aerospace field generally have a relatively high rotational speed, a relatively harsh working environment, and a relatively high performance requirement for a roller bearing. Currently, the relatively advanced aerospace gas turbine motor rotor DN is about $2x10^{-6}$ and the working temperature is about 200°C. The analysis of bearing deformation and rolling element load distribution under the action of radial force, axial force and force moment load was conducted [1-3]. A semi-dynamic model of the roller bearing was built, the load distribution and the pressure distribution of the contact area were analyzed, and the sliding rate of the cage and the motion speed of the roller contact surface were calculated [4, 5]. An analysis model of the high-speed flexible metal frame roller bearing was built, and the relationship between the deformation of the metal frame, the distribution of the received force inside the bearing, energy loss and the roller motion speed and the load distribution was studied [6]. A roller bearing dynamic model was created based on the fluid and elastic lubrication theory [7]. For roller bearings, a dynamic model was created assuming that the roller element has 6 degrees of freedom, the cage has 3 degrees of freedom, and the inner ring has 5 degrees of freedom [8]. The effects of radial load, working rotation speed, free clearance and roller number of rolling bearings on the roller motion rules were analyzed, and a test study was conducted on the sliding of rollers and cage [9]. The analysis of roller bearings is carried out using a quasi -dynamic method, and a dynamic model of roller bearings is included, but it is relatively small [10]. Using the Hertz theory, a model for static analysis of ball bearings was built, and the relationship between the maximum load and the radial load of the steel ball was derived [11] . A static analysis model for ball bearings was built, and the deformation and ball load distribution were analyzed under the action of radial loads, axial loads and force moment loads for the ball bearings [12]. A model for dynamic analysis of ball bearings subjected to arbitrary force was created using a quasi -dynamic method, and the motion state of each bearing part was determined by using the method of solving nonlinear equations [13]. In this paper, based on a specific study and analysis of the preceding literatures, the method of making a dynamic analysis model of high-speed roller bearings was specifically mentioned.

II. Theoretical Basis for Modelling

2.1 Establishment of coordinate system

1) Inertial coordinate system

Let the origin 0 of the inertial cartesian coordinate system be located at the center of the trajectory park of the curvature center of the outer roller groove, X axis coincides with the symmetric axis of the outer ring (the axis of the bearing), Z axis is along the direction of the radial load, and the axis is determined by X axis and Z axis through the right hand rule. This coordinate system is fixed in space. The origin of the inertial cylindrical coordinate system is the same as that of the inertial rectangular coordinate system. The direction of the polar radius of the coordinate system is the same as the Z axis in the rectangular system, the polar Angle is the Angle between the vector and the 2 axes in the rectangular system, and the height direction is the direction of the X axis in the rectangular system. The translational motion of all parts is determined in an inertial coordinate system. In general, the center of mass motion of the ring and cage is described in the inertial rectangular frame, and the center of mass motion of the ball or roller is determined in the inertial cylindrical frame.

(2) Definitive body coordinate system

The origin of the definite coordinate system is located at the center of mass of the part.The orientation of the coordinate axis of the relative coordinate system is consistent with the spindle of the bearing parts. The rotation of the part is determined by the rotation of the body coordinate system of the part relative to the inertial frame.

(3) Local coordinate system

In order to analyze the force, velocity and so on, we need to establish a local coordinate system. The origin of the local coordinate system is located at the center of the interface under investigation.The axes of the coordinate system are determined by local features.

2.2 Coordinate system analysis of roller bearing

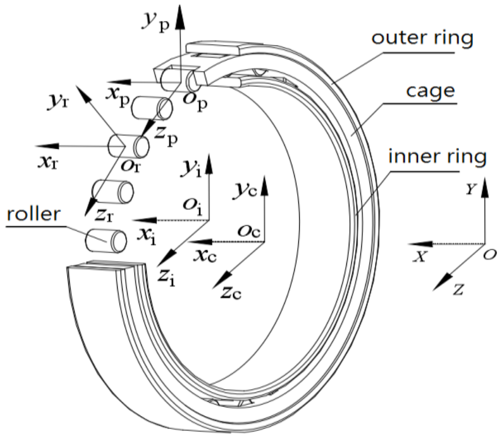

Figure1. Coordinate system of roller bearing

Inertial coordinate system of bearings $\{o; x, y, z\}$
Center coordinate system of roller$\{o_r;\ x_r, y_r, z_r\}$
Mass center coordinate system of cage$\{o_c;\ x_c, y_c, z_c\}$
Mass center coordinate system of Inner ring$\{o_i;\ x_i, y_i, z_i\}$
Mass center coordinate system of cage pocket$\{o_p;\ x_p, y_p, z_p\}$

2.3 HERTZ contact theory

~ Line contact

Roller bearings are generally linear contact, the surface pressure can be considered to be approximately semi-elliptical cylinder distribution.

The maximum compressive stress at the center of the contact width is;

$$\mathrm{P}_H = \frac{2q}{\pi b} = \left(\frac{qE'}{2\pi R}\right)^{0.5} = \frac{E'b}{4R} \quad (1)$$

The compressive stress at any point above is;

$$\mathrm{P} = \mathrm{P}_H\left(1 - \frac{y^2}{b^2}\right)^{0.5} \quad (2)$$

~ Point contact

The contact between the ball and the raceway is generally point contact, and the surface pressure can be considered to be approximately ellipsoid distribution. Under the action of load, a rectangular contact surface with a long half-axis of a and a short half-axis of b is formed.

When the short axis direction of the contact ellipse is reunited with the Y-axis, the contact stress p is;

$$\mathrm{P} = \mathrm{P}_H\left(1 - \frac{y^2}{a^2} - \frac{y^2}{b^2}\right) \quad (3)$$

The maximum Hertz contact stress P_H is;

$$\mathrm{P}_H = \frac{3Q}{2\pi ab} \quad (4)$$

2.4 High speed rolling bearing lubrication

When the bearing rotates at high speed, a lot of heat is produced. At this time, heat is generated from two sides. The first is the friction heat generated by the rotating movement of the bearing and the friction inside the component itself. The other is the stirring heat formed by the stirring effect of the component on the lubricant during high-speed rotation. Lubricants here have two main tasks: one is to play a lubrication role, when the bearing is working, it is required to continuously inject enough oil between the two contact surfaces to form a certain oil film thickness, so as to avoid direct contact between the two contact surfaces. The other is to play a cooling role, so that the temperature is maintained in the bearing materials and lubricating oil can withstand the range. The circulating pressure oil supply system with oil tank and oil pump makes the lubricating oil flow, and the heat exchange device can be used to effectively enhance the heat dissipation capacity of the bearing system.

III. Dynamic modelling for high-speed rolling bearings

3.1 Basic Assumptions

- Assume that the bearing parts are rigid bodies, and ignore the flexible deformation.
- The roller has five degrees of freedom: the revolution of the center of mass of the roller, the radial movement along the y_r-axis and the z_r-axis,

the rotation of the roller about the x_r-axis of its own center, and the tilt and skew of the roller.

- The cage has five degrees of freedom: the translational movement of the mass center of the cage along the y_c-axis and the z_c-axis in the radial $y_c z_c$ plane, the rotation about the y_c-axis and the z_c-axis, and the rotation of the mass center of the inner ring around the x_c-axis.

- The inner ring has five degrees of freedom: the translational motion of the center of mass of the inner ring along the y_i-axis and the z_i-axis in the radial $y_i z_i$ plane, the rotation about the y_i-axis and the z_i-axis, and the rotation about the center of mass of the inner ring around the x_i-axis.

3.2 Roller force analysis

High speed roller bearings are usually lubricated with lubricating oil. The outer ring of the bearing is fixed, the inner ring rotates, there is a pure radial force acting on the bearing, and the cage is guided by the outer ring.

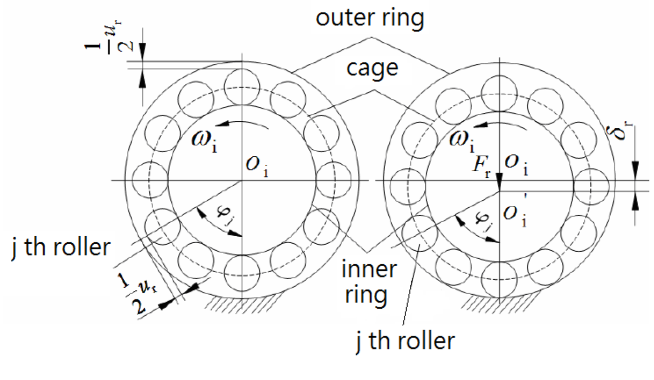

ㄱ) Before work ㄴ) After work

Figure 2. Schematic Diagram of Roller Bearings

In figure2, $0_i, o_i'$ is the center position of the inner ring of the bearing before and after working respectively; φ_j is the azimuth Angle of the jth roller; δ_r is the radial displacement of the inner ring; F_r is the radial force borne by the inner ring of the bearing.

① Schematic Diagram of roller force analysis

In the working process of the bearing, the roller is under the joint action of internal and external raceway, cage and lubricating oil, and the force of the roller is shown in Figure 3.

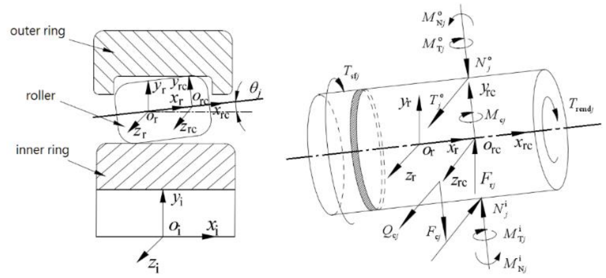

Figure 3. Schematic Diagram of roller force analysis

In Figure3, o_{rc} is the center of mass of the modified roller; o_r is the center of the roller axis; $\{o_{rc}; x_{rc}, y_{rc}, z_{rc}\}$ is the centroid coordinate system of the modified roller; θ_j is the inclination Angle of the roller; N_j^i , N_j^0 are the normal contact forces between the inner and outer raceways and rollers respectively; T_j^i , T_j^0 are the oil film drag force between the inner and outer raceway and the roller respectively; M_{Nj}^i , M_{Nj}^0 are the additional torques generated by the contact force between the inner and outer raceways and rollers respectively; M_{Tj}^i, M_{Tj}^0 are the additional torque generated by the oil film drag force between the inner and outer raceway and the roller respectively; Q_{cj} , F_{cj} are the normal contact force and tangential friction force between the cage beam and the roller; M_{cj} is the additional torque generated by the contact force between the roller and the cage beam; F_{rj} is the centrifugal force of the jth roller; T_{sfj} , $T_{ren\,dj}$ are respectively the surface blocking moment and end face blocking moment of lubricant on the jth roller.

② Analysis of force between roller and raceway

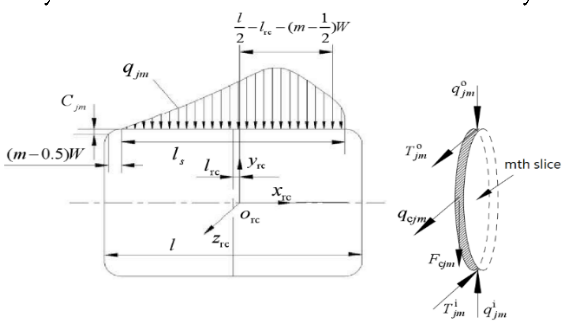

Figure 4. Schematic diagram of force on roller slice

The roller is evenly divided into NP segments along its own axis direction.

In Figure 4, W- slice width (W= l /NP)

l_{rc}-distance between the axial center of roller and the center of mass of roller

q_{jm}^{i}, q_{jm}^{0}-contact forces between the mth section of the jth roller and the inner and outer raceways respectively

T_{jm}^{i} ,T_{jm}^{0} -oil film drag force between the mth section of the jth roller and the inner and outer raceways respectively

Q_{cjm} , F_{cjm}- normal contact force and tangential friction force between the mth slice of the jth roller and the cage beam

The elastic deformation of the mth slice of the jth roller at the azimuth angle φ_j and the inner and outer raceways can be expressed as:

$$\begin{cases} \delta_{jm}^{i} = \delta_r \cos\varphi_j - \delta_j^{i} - \frac{u_r}{2} - C_{jm} \\ \delta_{jm}^{0} = \delta_j^{0} - C_{jm} \end{cases} \tag{5}$$

where δ_j^{i}, δ_j^{0}- Central deformation of the roller

C_{jm}- Reduction of the crown of the mth slice of the jth roller

The normal contact force between the jth roller and the inner and outer raceways can be expressed as:

$$\begin{cases} N_j^{i} = \sum_{m=1}^{NP} q_{jm}^{i} = \sum_{m=1}^{NP} \left(\delta_{jm}^{i}\right)^{1.11} \frac{W}{f^{1.11} l_s^{0.11} A^{1.11}} \\ N_j^{0} = \sum_{m=1}^{NP} q_{jm}^{0} = \sum_{m=1}^{NP} \left(\delta_{jm}^{0}\right)^{1.11} \frac{W}{f^{1.11} l_s^{0.11} A^{1.11}} \end{cases} \tag{6}$$

where A-Coefficient between the elastic deformation and the external load, A=1.36$\eta^{0.9}$(η- Comprehensive elastic constant of the two contact bodies)

f- Correction coefficient of improved sectioning method

The additional torque generated by the contact force between the inner and outer raceways and the jth roller can be expressed as:

$$\begin{cases} M_{Nj}^{i} = \sum_{m=1}^{NP} q_{jm}^{i} (\frac{l}{2} - (m - \frac{1}{2})W \pm l_{rc}) \\ M_{Nj}^{0} = \sum_{m=1}^{NP} q_{jm}^{0} (\frac{l}{2} - (m - \frac{1}{2})W \pm l_{rc}) \end{cases} \tag{7}$$

The oil film drag force of the jth roller by the inner and outer raceways can be expressed as:

$$\begin{cases} T_j^{i} = \sum_{m=1}^{NP} q_{jm}^{i} \mu_{jm} \\ T_j^{0} = \sum_{m=1}^{NP} q_{jm}^{0} \mu_{jm} \end{cases} \tag{8}$$

where μ_{jm}-Oil film drag coefficient between the mth section of the jth roller and the raceway

The additional torque of the jth roller due to the oil film drag force can be expressed as:

$$\begin{cases} M_{Tj}^{i} = \sum_{m=1}^{NP} q_{jm}^{i} \mu_{jm} (\frac{l}{2} - (m - \frac{1}{2})W \pm l_{rc}) \\ M_{Tj}^{0} = \sum_{m=1}^{NP} q_{jm}^{0} \mu_{jm} (\frac{l}{2} - (m - \frac{1}{2})W \pm l_{rc}) \end{cases} \tag{9}$$

③ Force between roller and cage

Contact model of roller and cage beam is follow:

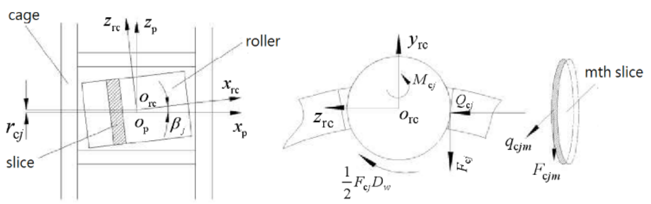

Figure 5. Contact model of roller and cage beam

The contact deformation of δ_{cjm} between the mth section of the jth roller and the cage beam can be expressed as[14]:

$$\begin{cases} \delta_{cjm} = |r_{cj}| - X_m \tan(\beta_j) - C_{jm} & r_{cj} \le CP \\ \delta_{cjm} = 0 & r_{cj} > CP \end{cases} \tag{10}$$

Where r_{cj}-Tangential distance between the jth roller and the cage pocket center

$X_m = \frac{l}{2} - (m - 0.5)W \pm l_{rc}$

β_j-Skew angle of the jth roller

CP-Circumferential clearance of cage pocket.

The contact force Q_{cj} between the jth roller and the cage beam can be expressed as:

$$Q_{cj} = \begin{cases} 0 & (\delta_{cjm} \leq 0) \\ \sum_{m=1}^{NP} Q_{cjm} = \sum_{m=1}^{NP} (\delta_{cjm})^{1.11} \frac{W}{f^{1.11} l_s^{0.11} A^{1.11}} & (\delta_{cjm} > 0) \end{cases} \quad (11)$$

The tangential friction between the cage beam and the jth roller can be expressed as:

$$F_{cj} = \sum_{m=1}^{NP} \mu_{cjm} Q_{cjm} \quad (12)$$

Where μ_{cjm}-Friction coefficient between the roller and the cage beam

The additional torque between the jth roller and the cage beam due to the contact force can be expressed as:

$$M_{cj} = \sum_{m=1}^{NP} q_{cjm} (\tfrac{1}{2} - \left(m - \tfrac{1}{2}\right) W \pm l_{rc}) \quad (13)$$

④ Viscous resistance of lubricating oil on roller

The viscous resistance of a roller is simulated by using the resistance of a cylinder when it moves in a fluid. When the cylinder is translational in the fluid, the resistance is:

$$F_\eta = -\operatorname{sign}(V) \cdot \frac{1}{2} C_D \rho V^2 S \quad (14)$$

where F_η: resistance

C_D: drag coefficient

ρ: equivalent density of the fluid

V: translational velocity of the cylinder

S: area of the cylinder in the direction of translation

For roller bearings:

$$S = L(D - L_e) \quad (15)$$

Where L: length of roller

D: diameter of the roller

W: thickness of the cage

The drag coefficient of the cylinder, C_D, is determined by the Reynolds coefficient, N_{RE}. Reynolds number N_{RE} is defined as:

$$N_{RE} = \frac{\rho V D}{\eta} \quad (16)$$

Where η: dynamic viscosity of the fluid

ρ: equivalent density of the fluid

It is the oil-gas mixture that is effective in the resistance. The viscosity of the oil is taken as the equivalent viscosity of the mixture when calculating the viscous resistance, and the equivalent density is determined by the ratio of the volume of the lubricating oil to the volume of the cavity.

$$\rho = \rho_{oil}\varepsilon_{oil} + \rho_{air}(1 - \varepsilon_{oil}) \quad (17)$$

where ρ_{air}, ρ_{oil}: densities of lubricating oil and air

ε_{oil}: percentage of the volume of lubricating oil in the cavity

⑤ Retardation torque of the lubricating oil on the roller

The total retardation torques acting on the surface and end face of the roller can be obtained by multiplying the radius of the roller by the shear stress on the surface and end face of the cylindrical roller respectively.

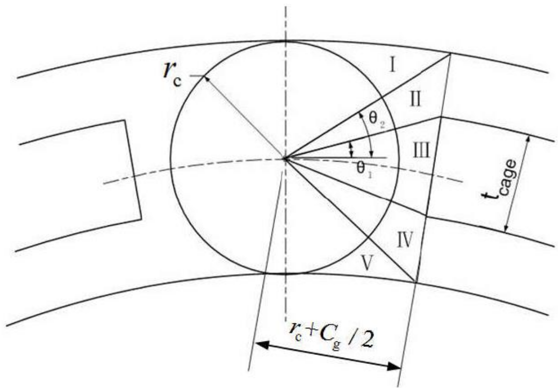

Figure 6. Calculation model of average clearance between roller and cage pocket

Calculate the average clearance at positionsI,II,IV and V in Figure 6.

The average gap is defined as follows:

$$C_H = \frac{1}{2\pi - 4\theta_2} \int C(\theta) d\theta \quad (18)$$

Furthermore, the average gap can be expressed as:

$$C_H = 2\left[r_c\left(ln\sqrt{\frac{1+\sin\theta_1}{1-\sin\theta_1}} - \theta_1\right) + \left(\frac{r_c+\frac{1}{2}C_g}{2}\right)\left(ln\frac{1+\cos\theta_1}{1-\cos\theta_1} - ln\frac{1+\sin\theta_2}{1-\sin\theta_2}\right) - r_c\left(\frac{\pi}{2} - \theta_1 - \theta_2\right)\right]/(\pi - 2\theta_2) \quad (19)$$

Where C_g- total circumferential clearance between the roller and cage pocket as shown in Figure 6.
r_c- Characteristic radius of the cage, which is equal to the non-guide surface radius of the cage.
ω_c-actual angular velocity of the cage
θ_1, θ_2-as shown in Figure 6

The shear stress on the roller surface is:

$$\tau_w = \frac{1}{2} f_c \rho_{eff} \left(\frac{r_c \omega_{rj}}{2}\right)^2 \quad (20)$$

Where ρ_{eff}- effective density of the oil-gas mixture around the roller

$$\frac{f_c}{f_L} = 1.3\left(\frac{N_{TA}}{41}\right)^{0.539437}$$

Friction coefficient of the wafer is:

$$f_L = 16/N_{RE}$$

Taylor number is:

$$N_{TA} = (r_c \omega_c C_H/\eta_0)\sqrt{C_H/r_c}$$

The average retardation torques on the roller surface is:

$$T_{sfj} = \tau_w r_c^2 l(2\pi - 4\theta_2) \quad (21)$$

3.3 Force analysis of cage

In the process of high-speed operation, the cage is affected by the impact force of the roller, the guide force of the outer ring, and the surface resistance and end resistance of the cage caused by the mixture of oil and gas.

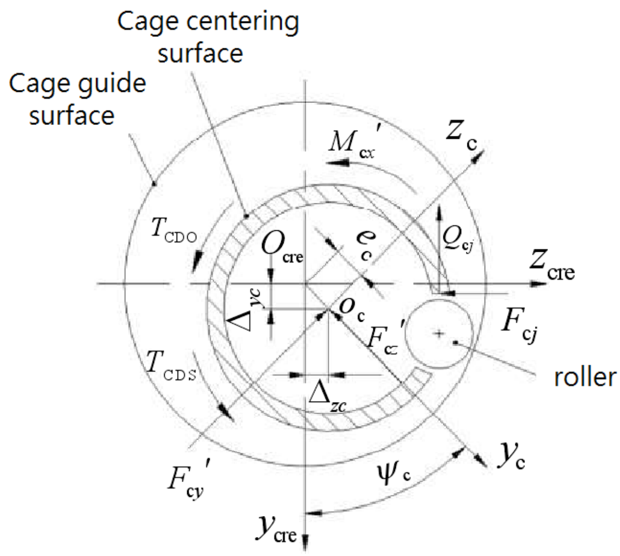

Figure 7. Schematic diagram of cage force

In Figure 7, $\{o_{cre}; x_{cre}, y_{cre}, z_{cre}\}$- reference coordinate system of the cage
e_c-relative offset of the cage center

$$e_c = \sqrt{\Delta_{yc}^2 + \Delta_{zc}^2} \quad (22)$$

where Δ_{yc}, Δ_{zc}- components of e_c on y_{cre} and z_{cre} axes respectively
ψ_c- included angle in the radial plane between the cage reference coordinate system $\{o_{cre}; x_{cre}, y_{cre}, z_{cre}\}$ and the cage coordinate system $\{o_c, y_c, z_c\}$

① Force between cage and guide ring

According to the geometric characteristics of the cage and the guiding outer ring, the two orthogonal components F_{cy}' and F_{cz}' acting on the cage due to the hydrodynamic pressure effect can be expressed as:

$F'_{cy} = \eta_0 u_1 L_c \varepsilon / [C_1^2 (1-\varepsilon^2)^2]$ (23)

$F'_{cz} = \pi \eta_0 u_1 L_c^3 \varepsilon / \left[4 C_1^2 (1-\varepsilon^2)^{3/2}\right]$ (24)

where L_c- centering surface width of the cage

C_1- cage guiding clearance

ε- relative eccentricity of the cage center

u_1- dragging speed of the lubricating oil

The distributed pressure of the lubricating oil fluid dynamic pressure oil film also produces a certain friction torque M'_{cx} on the cage surface:

$M'_{cx} = 2\pi \eta_0 V_1 R_{cd} L_c / \left(C_1 \sqrt{1-\varepsilon^2}\right)$ (25)

where V_1-relative sliding speed of the guiding surface and the centering surface

The forces F'_{cy}, F'_{cz} and moment M'_{cx} are calculated in the $\{o_c;\ x_c, y_c, z_c\}$ coordinate system. When establishing the dynamic differential equation of the cage, these forces and moments need to be converted to the inertial coordinate system$\{o; x, y, z\}$:

$$\begin{Bmatrix} M_{cx} \\ F_{cy} \\ F_{cz} \end{Bmatrix} = \begin{bmatrix} 1 & 0 & 0 \\ 0 & \cos\Psi_c & \sin\Psi_c \\ 0 & -\sin\Psi_c & \cos\Psi_c \end{bmatrix} \begin{Bmatrix} M'_{cx} \\ F'_{cy} \\ F'_{cz} \end{Bmatrix} \quad (26)$$

where $\psi_c = arctan(\Delta z_c / \Delta y_c)$

② Cage surface and end face resistance

The surface and end face of the cage are also subjected to the resistance action of the surrounding oil and gas mixture, and the blocking torque of the cylinder surface of the cage is T_{CDO} and the blocking torque of the cage end face is T_{CDS}.

$T_{CDO} = \tau A_{cage} r_{cage}$ (27)

$T_{CDS} = \frac{1}{2} \rho_{eff} \omega_c^2 r_{cage}^5 C_N$ (28)

$$C_N = \begin{cases} \frac{3.87}{(N_{RE})^{1/2}}, & N_{RE} \le 30000 \\ \frac{0.146}{(N_{RE})^{1/5}}, & N_{RE} > 30000 \end{cases} \quad (29)$$

Where A_{cage}- surface area of the cylindrical surface outside the cage

r_{cage}-radius of non-guiding surface of cage

τ- shear stress on the cylindrical surface of the cage

3.4 Nonlinear dynamic differential equations of high-speed roller bearings

According to the interaction force and motion state of each part of the bearing and Newton's second law, the nonlinear dynamic differential equations of each part of the high-speed cylindrical roller bearing are established respectively.

(1) Nonlinear dynamical differential equations of rollers

$$\begin{cases} m_b \ddot{y}_{bj} = -N_j^i \cos\varphi_j + N_j^0 \cos\varphi_j - Q_{cj} \sin\varphi_j - F_{rj} \cos\varphi_j - T_j^i \sin\varphi_j + T_j^0 \sin\varphi_j - F_{cj} \cos\varphi_j \\ m_b \ddot{z}_{bj} = N_j^i \sin\varphi_j - N_j^0 \sin\varphi_j - Q_{cj} \cos\varphi_j + F_{rj} \sin\varphi_j - T_j^i \cos\varphi_j + T_j^0 \cos\varphi_j + F_{cj} \sin\varphi_j \\ J_{bx} \dot{\omega}_{bx} = -T_j^i \frac{D_w}{2} - T_j^0 \frac{D_w}{2} + F_{cj} \frac{D_w}{2} \\ J_{by} \dot{\omega}_{by} = -M_{Tj}^i \sin\varphi_j - M_{Tj}^0 \sin\varphi_j + M_{cj} \cos\varphi_j + M_{Nj}^i \sin\varphi_j + M_{Nj}^0 \sin\varphi_j \\ J_{bz} \dot{\omega}_{bz} = -M_{Tj}^i \cos\varphi_j - M_{Tj}^0 \cos\varphi_j - M_{cj} \sin\varphi_j + M_{Nj}^i \cos\varphi_j + M_{Nj}^0 \cos\varphi_j \end{cases} \quad (30)$$

Where m_b- mass of the roller

$\ddot{y}_{by}$, $\ddot{z}_{by}$ - displacement acceleration of the center of mass of the jth roller in the inertial coordinate system $\{o; x, y, z\}$

J_{bx}, J_{by}, J_{bz} - moment of inertia of rollers in the inertial coordinate system$\{o; x, y, z\}$

$\dot{\omega}_{bx}$, $\dot{\omega}_{by}$, $\dot{\omega}_{bz}$-angular accelerations of the roller in the inertial coordinate system $\{o; x, y, z\}$

(2) Nonlinear dynamic differential equations of cage

$$\begin{cases} m_c\ddot{y}_c = \sum_{j=1}^{RN}\left(Q_{cj}\sin\varphi_j + F_{cj}\cos\varphi_j\right) + F'_{cy}\cos\Psi_c + F'_{cz}\sin\Psi_c - G_c \\ m_c\ddot{z}_c = \sum_{j=1}^{RN}\left(Q_{cj}\cos\varphi_j - F_{cj}\sin\varphi_j\right) + F'_{cy}\sin\Psi_c - F'_{cz}\cos\Psi_c \\ J_{cx}\dot{\omega}_{cx} = \sum_{j=1}^{RN}\left(F_{cj}\frac{D_w}{2}\right) - M'_{cx} - T_{CDO} - T_{CDS} \\ J_{cy}\dot{\omega}_{cy} = \sum_{j=1}^{RN}\left(-M_{cj}\cos\varphi_j\right) \\ J_{cz}\dot{\omega}_{cz} = \sum_{j=1}^{RN}\left(M_{cj}\sin\varphi_j\right) \end{cases} \quad (31)$$

Where m_c- mass of the cage

G_c-cage gravity

RN-number of rollers

$\ddot{y}_c$, $\ddot{z}_c$-centroid acceleration of the cage in the inertial coordinate system$\{o; x, y, z\}$

J_{cx}, J_{cy}, J_{cz} -moment of inertia of the cage in the inertial coordinate system$\{o; x, y, z\}$

$\dot{\omega}_{cx}$, $\dot{\omega}_{cy}$, $\dot{\omega}_{cz}$-angular accelerations of the cage in the inertial coordinate system$\{o; x, y, z\}$

(3)Nonlinear dynamical differential equations of inner ring

$$\begin{cases} \mathrm{m}_i\ddot{y}_i = \sum_{j=1}^{RN}\left(N_j^i\cos\varphi_j + T_j^i\sin\varphi_j\right) - F_r \\ \mathrm{m}_i\ddot{z}_i = \sum_{j=1}^{RN}\left(-N_j^i\sin\varphi_j + T_j^i\cos\varphi_j\right) \\ J_{ix}\dot{\omega}_{ix} = \sum_{j=1}^{RN} T_j^i\frac{D_w}{2} \\ J_{iy}\dot{\omega}_{iy} = \sum_{j=1}^{RN}(M_{Tj}^i\sin\varphi_j) \\ J_{iz}\dot{\omega}_{iz} = \sum_{j=1}^{RN}(M_{Tj}^i\cos\varphi_j) \end{cases} \quad (32)$$

Where m_i-mass of the inner ring

$\ddot{y}_i$, $\ddot{z}_i$-centroid acceleration of the inner ring in the inertial coordinate system$\{o; x, y, z\}$

J_{ix}, J_{iy}, J_{iz}- moment of inertia of the inner ring in the inertial coordinate system$\{o; x, y, z\}$

$\dot{\omega}_{ix}$, $\dot{\omega}_{iy}$, $\dot{\omega}_{iz}$-angular accelerations of the inner ring in the inertial coordinate system$\{o; x, y, z\}$

IV. DISCUSSION

The dynamic performance of high-speed roller bearing is not only related to the structural dimensions, machining precision, and material performance of bearing, but also related to factors such as working conditions, assembly precision, type of lubricants, and lubrication conditions.Therefore, based on referring to the theoretical basis for building the dynamic model of the high-speed roller bearing, an assumption for building the dynamic model was raised.First of all, in addition to the interactive force and force moment between each part of high-speed roller bearing, the centrifugal force, the viscosity resistance force on roller and the resistance force of cage end face and surface, it also considered the influence on the dynamic performance of machining error of the bearing, and specifically analyzed the influence of the working condition of the bearing and the roughness of the working surface on the lubrication condition of the bearing.In addition, on the basis of the dynamic simulation model of the already existing high-speed roller bearing, a dynamic model of the high-speed roller bearing was built, which specifically considered the contact condition and the lubrication condition of the bearing.

V. CONCLUSION

High-speed roller bearing is widely used as a supporting part of rotating machines due to its high speed performance and low friction moment. As rotating machinery is developing towards the aspects of high-speed, high precision and high reliability, the research on the dynamic performance of high-speed roller bearing is becoming more important. In this paper, an analysis of the interaction relationship between the position of each part of the high-speed roller bearing was conducted and the influence of factors such as resistance was considered. By applying Hertz theory, elastic liquid and hydrodynamic theory, a specific analysis was conducted on the force and movement of every part inside the roller bearing. The kinematics equations of each part were established by analyzing specifically the relationship between roller and the road, the relationship between roller and the cage, the viscosity resistance and the oil film resistance. Based on these equations, the nonlinear dynamics model of the high-speed roller bearing was established. The dynamic model of the high-speed roller bearing provides a theoretical basis for the analysis of the dynamics performance, design and calculation of the coefficient for the high-speed roller bearing.

VI. REFERENCES

[1]. ELundberg G, Palmgren A. Dynamic capacity of rolling bearings J Acta Polytechnica. Mechanical Engineering Series, 1947, 1(3): 5-50.

[2]. Lundberg G, Palmgren A. Dynamic capacity of roller bearings J Acta Polytechnica. Mechanical Engineering Series, 1952, 2(4): 96-127.

[3]. Palmgren A. Ball and roller bearing engineering M 3rd ed. Philadelphia: Burbank, 1959.

[4]. Cretu S, Bercea I, Mitu N. A dynamic analysis of tapered roller bearing under fully flooded conditions Part 1: theoretical formulation J Wear, 1995, 188(1-2): 1-10.

[5]. Cretu S, Mitu N, Bercea I. A dynamic analysis of tapered roller bearings under fully flooded conditions Part 2: results J Wear, 1995, 188(1-2): 11-18.

[6]. Cavallaro G, Nelias D, Bon F. Analysis of High-Speed Intershaft Cylindrical Roller Bearing with Flexible RingsJ Tribology Transactions, 2005, 48(2): 154-164.

[7]. Conry T F, Goglia P R. Transient dynamic analysis of high-speed lightly loaded lylindrical roller bearings. II -- Computer program and results, NASA Contractor Report 3335R], 1981.

[8]. JAFAR TAKABI, M. M. KHONSARI. On the Influence of Traction Coefficient on the Cage Angular Velocity in Roller Bearings J Tribology Transactions, 2014.57(5):793-805.

[9]. Gupta P K. On the dynamics of a tapered roller bearing J Journal of Tribology, Transaction of the ASME, 1989, 111(2): 278-287.

[10].Sakaguchi T, Harada K. Dynamic analysis of cage behavior in a tapered roller bearing J Journal of Tribology, Transaction of the ASME, 2006, 128(3): 604-611.

[11].Sakaguchi T, Kaoru U. Dynamic Analysis of Cage Behavior in a Cylindrical Roller Bearing J Special Issue Special Supplement to Industrial Machines, 2004.

[12].Conry T F. Transient dynamic analysis of high-speed lightly loaded lylindrical roller bearings. I-Analysis, NASA Contractor Report 3334R], 1981.

[13].Gupta P K, Dill J F, Bandow H E. Dynamics of rolling element-bearings experimental validation of the DREB and RAPIDREB computer programs J Journal of Tribology, Transaction of the ASME.1985, 107: 132-137.

[14].Yang H S, Cheng G D, Deng S E, et al. Analysis of the roller-race contact deformation of cylindrical roller bering using a improved slice methodCInternational Conference on Mechatronic Science, Electric Engineering and Computer. IEEE, 2011:711-714.

Cite this article as :

CholUk Ri, ZhunHyok Zhang, WonRyong Pak, JaeHun Kim ,IlSon Yun, CholMin Han, JongMin Han , "A Study on the Dynamic Analysis Modelling for High-Speed Roller Bearings",International Journal of Scientific Research in Mechanical and Materials Engineering (IJSRMME), ISSN : 2457-0435, Volume 5 Issue 1, pp. 01-10, January-February 2021.

URL : http://ijsrmme.com/IJSRMME21512